

PAPER • OPEN ACCESS

## Prediction of vibration amplitudes on hydraulic profiles under von Karman vortex excitation

To cite this article: B Nennemann and C Monette 2019 *IOP Conf. Ser.: Earth Environ. Sci.* **240** 062004

View the [article online](#) for updates and enhancements.

### Recent citations

- [FSI analysis of francis-99 hydrofoil employing SBES model to adequately predict vortex shedding](#)  
P upr *et al*

# Prediction of vibration amplitudes on hydraulic profiles under von Karman vortex excitation

**B Nennemann and C Monette**

ANDRITZ HYDRO Canada Inc.,  
6100 aut. transc., H9R 1B9, Pointe-Claire, Canada

E-mail: bernd.nennemann@andritz.com

**Abstract.** The shedding of von Karman vortices on the trailing edges of turbine hydraulic profiles such as stay vanes, guide vanes and runner blades is a well-known mechanism of excitation for high frequency structural vibrations. Most commonly problems occur on stay vanes because the flow across the trailing edges is relatively uniform, and structural damping is low. Our analysis of the excitation mechanism under von Karman vortex shedding shows that in the vicinity of resonance the hydrodynamic damping becomes a non-linear function of amplitude potentially resulting in unacceptable limit amplitudes. Past studies have focused on frequency prediction, resonance avoidance and special trailing edge shapes to reduce dynamic forcing. On modern low head turbines resonance cannot always be avoided without undue hydraulic performance penalties. In our paper we demonstrate the applicability of a fluid structure interaction based approach to predict vibration amplitudes under von Karman vortex shedding. This type of prediction can be used to ensure that permissible amplitudes are not exceeded. We also present a strategy to achieve low vibration amplitudes.

## 1. Introduction

Vortex shedding behind cylinders and bluff bodies has been widely studied and is well summarized in text books on flow induced vibrations e.g. [1][2] where references to the original literature can be found. Vortex shedding as a source of unacceptable vibrations or noise in hydraulic turbines has been reported as early as 1956 by Donaldson, e.g. quoted in [3]. It is reported to occur on turbine runner blades e.g. [4] and to the author's knowledge only in one case on guide vanes [5]. Most commonly, it occurs on stay vanes because the flow across stay vane trailing edges is relatively uniform, and structural damping is low. An excellent review of stay vane cracking as a result of vortex shedding is given in [6]. A well-documented specific case is documented in [7]. A summary on all turbine related vortex shedding can also be found in [8]. Two relatively recent PhD theses [9][20] have added new experimental data and insights.

Most of the existing literature has focused on frequency prediction, resonance avoidance and counter-measures, reducing or eliminating dynamic forcing from vortex shedding. Our paper investigates the mechanisms influencing vibration amplitudes and presents a methodology to predict the latter. A strategy to avoid unacceptable vibration amplitudes without avoiding resonance is also given.

## 2. Vortex shedding and frequency prediction

An example of a vortex street visualized in a laboratory experiment by means of cavitation is shown in figure 1. Figure 2 shows vortex shedding behind the trailing edge of a stay vane visualized by z-vorticity from an unsteady CFD (Computational Fluid Dynamics) simulation. Essentially, vortex formation is the



result of a shear layer instability, resulting in its rolling up. Von Karman formulated the vortex street problem as two rows of potential vortices with opposing sense of rotation. Using a potential flow formulation and linear stability analysis von Karman could show that the only possible configuration of such rows of vortices was an alternating one with a specific geometric configuration, e.g. [2]. The theoretical ratio of the distance of vortex centers  $t_w$  to vortex spacing in the same row  $l_{vK}$  has to be  $t_w/l_{vK} \approx 0.281$ . Karman's theory made no prediction about the shedding frequency.

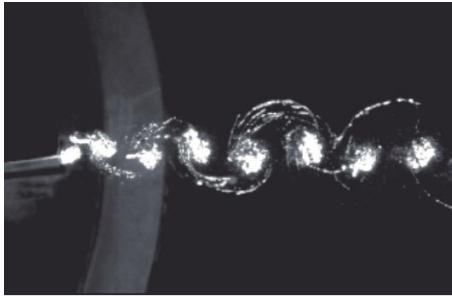


**Figure 1.** Vortex shedding behind a NACA0009 profile visualized by cavitation from [9].

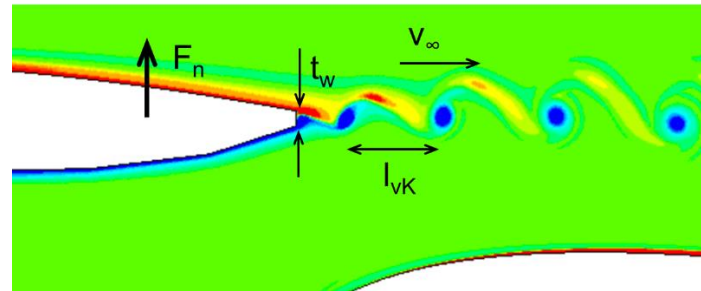


**Figure 2.** Vortex shedding behind a stay vane trailing edge in CFD z-vorticity (red -2000/s, blue 2000/s), definitions.

Experimental results show that the shedding frequency  $f_{vK}$  follows the well-known Strouhal-relationship

$$f_{vK} = S_h \cdot \frac{v_\infty}{t_w} \quad (1)$$

with Strouhal number  $S_h$ , the effective free stream velocity  $v_\infty$  and the effective wake thickness  $t_w$ . A flow rate based theoretical value can be a reasonable estimate for  $v_\infty$ , but in many cases effects such as the proximity of the guide vane near full opening can have a significant effect of up to 20% on the shedding frequency. Using a purely geometric value for  $t_w$  will result in a large spread of Strouhal number. A better estimate of the wake thickness may be obtained using boundary layer theory, but we believe that steady state viscous CFD is the best approach to obtain a reasonably reliable estimate of the shedding frequency based on the Strouhal number. From a velocity profile at the trailing edge obtained by steady state viscous CFD the effective velocity  $v_\infty$  and the effective wake thickness  $t_w$  can be extracted. We found the wake thickness obtained by a velocity cut off at  $\approx 0.48v_\infty$  to yield the best results. This method can be used on any hydraulic profile.

Unsteady CFD can predict vortex shedding frequencies with good accuracy [10]. Accuracy has still been improved to about  $\pm 10\%$  (figure 6). Figure 3 demonstrates the scatter of the Strouhal number for 14 stay vane designs at multiple flow velocities and inflow angles each calculated with unsteady CFD. The scatter becomes narrower as the Reynolds number increases. Round trailing edges as well as very low Reynolds numbers are the two factors that account for the largest deviations from a near constant Strouhal number. The best average value for a Strouhal number to estimate a shedding frequency is  $S_h \approx 0.2$ , but the limitations of a Strouhal number based approach are clear from the graph.

### 3. Dynamic Force prediction

#### 3.1. Analytical

Heskestad [3] derived an analytical equation for the dynamic force on a stay vane resulting from vortex shedding. The derivation is based on von Karman's ratio of wake to vortex spacing and potential flow theory to obtain the circulation. The latter is then used in Kutta-Joukowski's relation for a force on a profile based on bound circulation. Using a ratio  $t_w/l_{vK} \approx 0.29$  and a Strouhal number of  $S_h \approx 0.2$  the equation for the dynamic force amplitude as a result of vortex shedding can be reduced to

$$F_{vK.ana} \approx 1.5 \frac{\rho}{2} B_0 t_w v_\infty^2 \quad (2)$$

with the stay vane height  $B_0$  and the fluid density  $\rho$ . The form of this equation is identical to any expression of a lift force on hydraulic or aerodynamic profiles where 1.5 would be the lift coefficient.

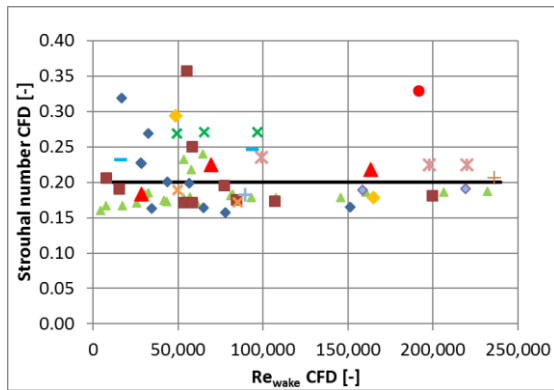


**Figure 3.** Strouhal number variation on stay vanes, frequency from unsteady CFD,  $t_w$  and  $v_\infty$  from steady CFD. Round symbols from a round trailing edge.

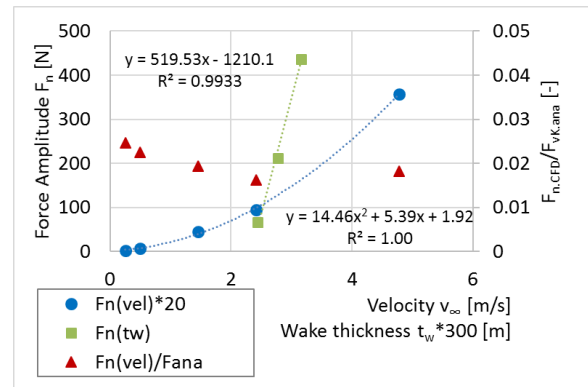


**Figure 4.** Unsteady CFD normal force amplitude on a stay vane as function of flow velocity  $F_n(\text{vel})$ , wake thickness  $F_n(\text{tw})$ , and CFD over analytical force from equation (2).

Equation (2) indicates that the dynamic force is proportional to the wake thickness  $t_w$  and to the square of the free stream velocity  $v_\infty$ . Figure 4 confirms these proportionalities with results obtained by unsteady 2D CFD. However, the ratio of the force amplitude from unsteady CFD over the analytical force from equation (2)  $F_n/F_{vK.ana}$  in figure 4 clearly shows that with a lift coefficient of 1.5 in equation (2) we greatly over-predict the dynamic force compared to unsteady CFD. In this example the over-prediction is with a factor of  $\approx 50$  but on other profiles it can be as low as 2. Equation (2) can therefore serve as an upper limit but is in general too constraining for practical purposes.

### 3.2. Numerical

Direct dynamic force measurements of good quality without fluid-structure coupling are difficult to perform in practice. We believe that numerical modelling with CFD is a good approach to predict the dynamic force from vortex shedding in cases where vortices are strong. The successful prediction of vibration amplitudes in section 6 indicates that the dynamic forcing is most probably be predicted with reasonable accuracy.

## 4. CFD modelling

Unlike some unsteady phenomena in hydraulic turbines such as rotor stator interaction, von Karman vortex shedding is the result of shear layer instability. It is therefore significantly more challenging numerically. Our CFD computations are performed with the commercial code ANSYS-CFX.

The computational mesh needs to be fine to adequately resolve the high gradients in the boundary layers that drive the vortex shedding and in the vortices themselves. A typical mesh for a stay vane-guide vane combination is shown in figure 5 consisting of about 360k nodes and  $y^+$ -values near 1. The basic approach for distributors is 2D, which has been proven to be fully sufficient for shedding frequency prediction [10][11]. Our results show that a 2D approach delivers an upper limit for the dynamic force amplitude compared to a 3D approach as one would expect. We use extruded hybrid hexahedral and prismatic meshes for vortex shedding because they permit strong local refinement where it is needed, i.e. in the wake and the boundary layer, without imposing refinement elsewhere.

Our standard numerical formulation uses a hybrid URANS-scale resolved approach with the SAS turbulence model. This has given good accuracy in the frequency prediction and results in largest force amplitudes compared with other two-equation turbulence models such as SST. Very slightly higher force amplitudes, and equally accurate frequency predictions have been achieved with an  $\omega$ -Reynolds stress model, but at close to double the computational cost and higher convergence problems.

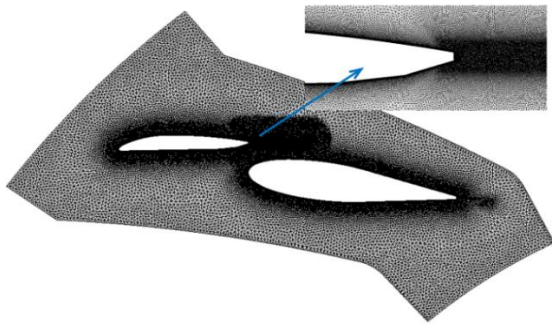


**Figure 5.** Typical mesh for prediction of stay vane vortex shedding: 360k nodes and resolution of boundary layer with  $y^+ \approx 1$ .

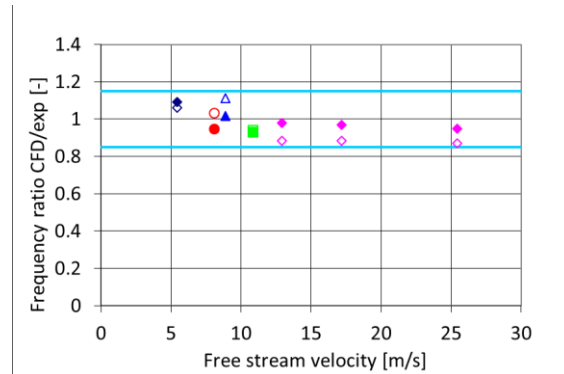


**Figure 6.** Predicted over measured vortex shedding frequencies on three stay vanes and Hydrodyna NACA0009 profile. Full symbols from unsteady CFD, open symbols calculated with steady state CFD input and  $S_h=0.2$ .

Small time steps, in the range of 200 to 400 per oscillation cycle, are required for good accuracy. The second order upwind advection scheme with a fixed blend factor of 1.0 in ANSYS is highly advisable for this application. While three to five coefficient loops are sufficient for frequency and force predictions, the modal work approach (section 6.1) requires a very high level of convergence with max residuals below 3 to 5e-6. Figure 6 shows a comparison of predicted and measured frequencies. The results from unsteady CFD fall within a band of  $\pm 10\%$ .

In the CFD based studies reported in the literature ([7], [11]-[14]), similar numerical approaches have been used. Two-equation turbulence models were tested in particular in early studies, but it became clear that more advanced turbulence options such as the hybrid SAS turbulence model or Reynolds stress models perform better for vortex shedding. When investigating trailing edges that were designed to generate low dynamic forcing, some authors even employed LES or DES approaches. Miyagawa *et al.* [11] achieved very good predictions of the shedding frequency using LES and found that 2D modelling achieved practically the same results as 3D modelling. D'Agostini [13] needed to resort to a DES approach with very fine meshes to predict vortex shedding on stay vanes of a Francis turbine that suffered recurring cracks when even the SAS turbulence model did not deliver realistic results.

So far we have had good results with fine hybrid meshes, SAS turbulence model, small time steps and high convergence levels.

## 5. Excitation mechanism under von Karman vortex shedding

It is understood that von Karman vortices can and will form on the trailing edges of almost all hydraulic profiles and therefore exert some degree of dynamic loading on the structure. On modern hydraulic profiles, with generally thin trailing edges, significant “excitation”, i.e. levels that lead to vibrations with either unacceptable noise or dynamic stress levels resulting in fatigue cracks, will only occur at or near resonance [6]. For unacceptable noise or fatigue cracks to occur, the natural shedding frequency has to be close to a natural frequency of the structure in water. Accurate prediction of natural frequencies in water has become well proven using standard finite element analysis (FEA) approaches, e.g. [19]. Resonance alone however does not explain the mechanism of excitation. In Naudascher [1] excitation due to vortex shedding is classified as “instability-induced excitation”, and can therefore not be treated

as a simple forced response. In fact, using the dynamic forcing from unsteady CFD without structural motion leads to very low effective damping to explain the amplitudes measured on turbine stay vanes. Structural damping alone is too low ( $\approx 0.03$ - $0.3\%$ ) to explain the measured vibration amplitudes, while typical hydrodynamic damping values (in the order of multiple % [15]- [18]) are too high.

Miyagawa [11] used 2-way modal fluid structure interaction (FSI) modelling to predict vibration amplitudes. In their study they determined the hydrodynamic damping as a function of reduced velocity, and identified a drop in damping, where the largest vibration amplitudes occur. They interpreted it such that *negative* damping can occur if no numerical damping were present, and that the high vibration amplitudes are therefore the result of a self-excitation.

A different or an additional hydrodynamic mechanism must then be present under von Karman vortex shedding. In the vorticity plots in figure 7, we can see that vortices are generated by the imposed modal motion. These resemble von Karman vortices as the wave length  $v/f$  approaches values similar to those found in Karman vortices. In the figure this is the case for a flow velocity of  $2\text{m/s}$ . Actual von Karman vortices are not present in these computations. Their frequencies would be well above the modal oscillation frequency. This means that at least one of the main mechanisms of transferring energy from the oscillating hydrofoil to the fluid (resulting in positive damping) resembles natural von Karman vortices. The decrease of hydrodynamic damping as the shedding frequency approaches a natural frequency of the structure can then be explained by this flow structure similarity.

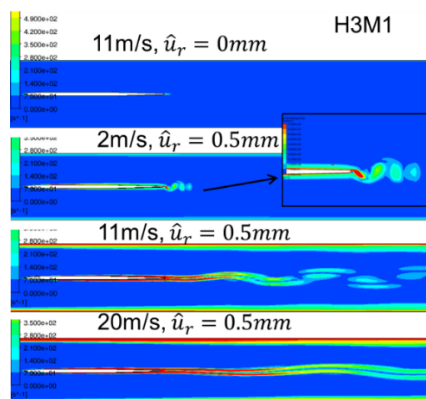


**Figure 7.** Three vorticity magnitude plots for damping plate H3 [16]-[17] with 1<sup>st</sup> bending mode imposed at 74Hz. Karman vortex shedding is not resolved in these computations but would be about 200Hz for 2m/s.  $\hat{u}_r$  is the modal reference amplitude.

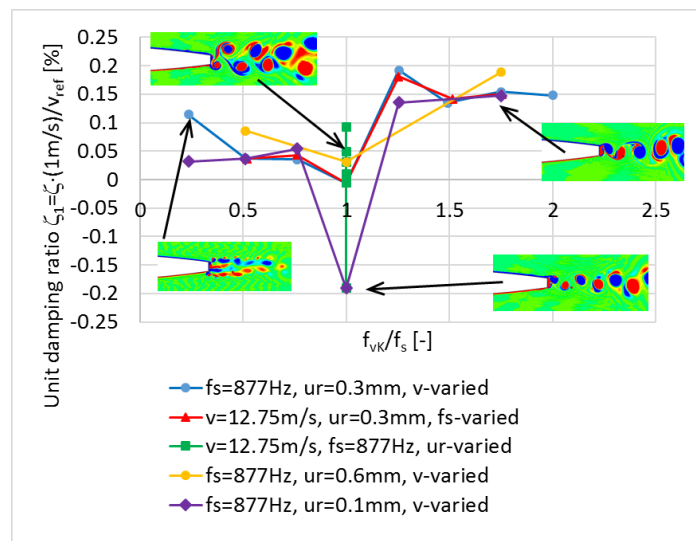


**Figure 8.** Modal work (section 6.1) results for Hydrodyna truncated NACA0009 profile at 1<sup>st</sup> torsion mode: Unit damping  $\zeta_1$  as function of von Karman over forcing frequency  $f_{vK}/f_s$ . Flow topology visualized by z-vorticity for selected flow conditions. Most important conclusion: hydro-dynamic damping becomes strong function of amplitude as  $f_{vK}/f_s \rightarrow 1$ .

The actual vibration amplitude of a hydrofoil under Karman vortex shedding is obtained, when energy transfer per cycle between structure and flow are in balance. The concept described under “Energy consideration” in [1] applies to this situation. However, here the excitation and the dissipation stem from a very similar flow structure. The system exhibits an apparent hydrodynamic damping  $\zeta_{vK}$  that is a function of the frequency ratio  $f_{vK}/f_n$  and the amplitude  $\hat{u}_r$  making the system non-linear  $\zeta_{vK} = f(\frac{f_{vK}}{f_n}, \hat{u}_r)$ . This is compatible with Miagawa’s [11] findings short of calling it self-excitation, and is

confirmed by figure 8. We introduce the unit damping ratio  $\zeta_1 = \zeta \cdot (1 \text{ m/s})/v_\infty$  (to eliminate the linear dependency of hydrodynamic damping on free stream velocity) and plot it against the ratio of von Karman over forcing frequency (imposed in CFD computation)  $f_{vK}/f_s$ . Many things can be learned from this figure: The results can be obtained either by varying the velocity or the forcing frequency (blue and red lines); the damping ratio is relatively independent of vibration amplitude below a certain threshold amplitude when von Karman resonance is *not* present (blue and purple lines); above a certain amplitude threshold the damping ratio becomes dependent on the amplitude everywhere (yellow vs blue lines), but this is for amplitudes beyond practical importance in turbines. Most importantly for von Karman vortex excitation: near  $f_{vK}/f_s=1$  the damping ratio becomes very strongly dependent on amplitude and varies from negative to positive values. This can also be seen in figure 11b (data correspond to green line in figure 8) where the strong non-linearity is also apparent. The amplitude at which a real system will vibrate is defined by  $\zeta=0$ . Note that damping shown in figure 8 represents hydrodynamic damping only.

A necessary condition for a mode to respond with a significant amplitude is the proximity of the exciting frequency to the natural frequency as in all resonance phenomena. In addition, positive hydrodynamic damping is only available above a certain vibration amplitude because the hydrodynamic phenomena of natural vortex shedding and energy dissipation from modal motion have a very similar character (hydraulic mode). As the vortex shedding frequency and the frequency of oscillation approach, the wave lengths of the respective vortices join. As vibration amplitudes increase, hydrodynamic damping does so until a limit amplitude is reached.

The two plateaus of near constant unit damping above and below a frequency ratio of 1 in figure 8 correspond to the findings by [18] where two slopes of velocity versus hydrodynamic damping were identified when von Karman vortex shedding was present. This means that we have different hydrodynamic damping at sub and super resonant conditions under von Karman vortex shedding. In experiments where the imposed oscillation was far from the Karman vortex shedding frequency, only a single slope was measured [15].

## 6. Vibration amplitude prediction

### 6.1. FSI modelling

Modal FSI modelling to predict vibration amplitudes under von Karman vortex shedding has been employed by [11] and [12]. Both use a similar approach, modelling the mode of interest as a single degree of freedom oscillator (1dof) and coupling it to the CFD solution. As a result one obtains the vibration amplitude directly. The same approach has also been used in the prediction of hydrodynamic damping e.g. [16][17] and for the prediction of flutter-type self-excitation on pump turbine guide vanes. An alternative is the approach we call *modal work approach* where the mode shape of interest is imposed in a harmonic motion with a given amplitude during a CFD computation, figure 9. In general it is a 3D approach. The energy (modal work) exchanged between the structure and the fluid is computed from:

$$W_{m,T} = - \int_0^T \int_A (p\underline{n} + \underline{\tau}) \cdot \underline{\dot{u}}_r(t) dAdt \quad (3)$$

with pressure  $p$ , surface normal  $\underline{n}$  (pointing into the fluid), wall shear  $\underline{\tau}$ , time  $t$ , oscillation period  $T$ , mode shape velocity  $\underline{\dot{u}}_r$ , structure surface area  $A$ , and underbars denoting vectors. Magnitude and sign are related to hydrodynamic damping. The modal work can be converted into an equivalent linear damping ratio  $\zeta$  for a given mode  $m$  by

$$\zeta_m = \frac{W_{m,T}}{2\pi m_m \omega_{nsw}^2 \hat{u}_r^2} \quad (4)$$

with the modal mass in water  $m_m$ , the modal natural angular frequency of the structure in water  $\omega_{nsw}$ , and the other symbols as before. The modal work  $W_{m,T}$  can be positive or negative. The sign can mean different things depending on the FSI system. In the context of a hydraulic profile under strong flow velocity in the absence of von Karman vortices it will generally be positive [15]. In the presence of von

Karman vortices, positive damping indicates that the natural vibration amplitude, i.e. the amplitude that will result as a consequence of energy balance, is smaller than the imposed amplitude. Conversely, if the damping is negative, the natural vibration amplitude will be larger than the imposed amplitude as in the example shown in figure 10 where the green line of the modal work per cycle drops below zero. In other situations, such as pump turbine guide vane flutter or air foil flutter, negative damping indicates self-excitation. In these cases no limit vibration amplitude of the system itself may exist, and a real system's amplitude may only be limited by non-linearity such as contact with a nearby structure.

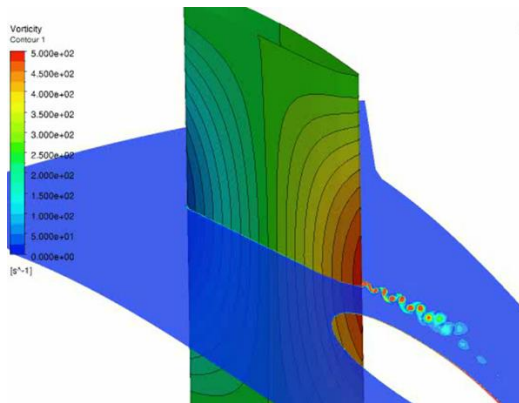


**Figure 9.** Imposed 1<sup>st</sup> torsion mode shape on a stay vane and concurrent vortex shedding. Colouring: displacement on vane (blue -0.2mm, red 0.2mm displacements normal to vane camber line), vorticity magnitude on mid-span plane.

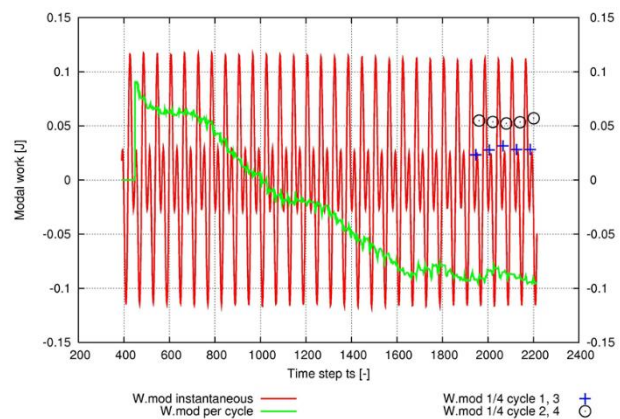


**Figure 10.** Modal work on a stay vane as function of time step for imposed amplitude of 0.2mm. Instantaneous value in red, summed over one period in green. At end of calculation  $W_{m,T} < 0 \Rightarrow$  natural vibration amplitude  $> 0.2mm$ .

The modal work approach has the advantage of being numerically robust, which is important in the light of the numerical challenges that von Karman vortex shedding poses. It is well suited for the situation of von Karman vortices where the hydrodynamic damping is a function of frequency and amplitude as well as flow velocity. The natural vibration amplitude is found by imposing a number of amplitudes for a given frequency, flow condition and eigen mode.

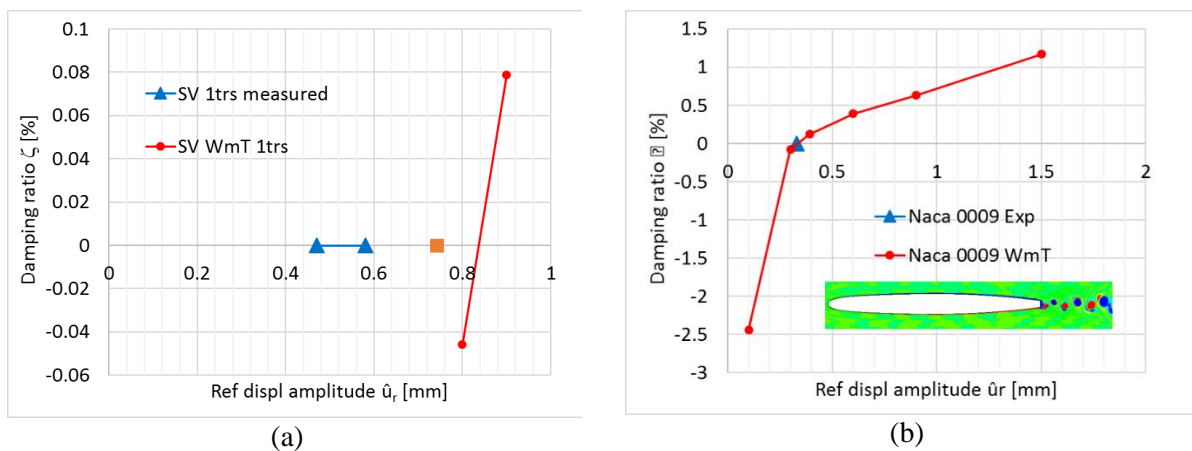


**Figure 11.** Measured and predicted vibration amplitudes of 1<sup>st</sup> torsion modes at von Karman resonance. (a) Stay vane: orange square is amplitude calculated from modal work corrected with measured structural damping in air. (b) Truncated NACA0009 profile from Hydrodyna project measured in laboratory, results reported in [20].

## 6.2. Validation

The red lines in figure 11 show the type of results one obtains from the modal work approach: modal work – which can optionally be converted to a damping ratio with equation (4) – varying from negative to positive values as a function of modal amplitude for a given frequency. The point where the modal work or corresponding damping ratios intersect zero defines the predicted vibration amplitude.

In the case of the stay vane, we see an over-prediction of the vibration amplitude, as one would expect if the modal work approach gave perfect results, because we are neglecting mechanical and acoustic damping. In this example structural damping in air was measured, and the orange square indicates the predicted amplitude including structural damping. Structural damping is generally very low in stay vanes. It is mode and case dependant. In the example for which we have measurements it varies between 0.03 and 0.3% for the different modes. Even when structural damping is considered we still see an over-prediction of about 30%. This may be due to acoustic damping or secondary effects not considered in the CFD. Inaccuracies in the transposition from measured strains to displacement amplitudes may also play a role. The level of over-prediction is acceptable and highly preferable over an under-prediction.

The truncated NACA0009 profile was measured in the Hydrodyna project. The vibration amplitudes used here for validation were read out of a figure in [20] and transposed to the maximum displacement with a linear relationship. Some inaccuracy regarding the measured value may stem from this approach. We see an exact prediction of the vibration amplitude while we would expect to see a slight over-prediction due to neglected structural and acoustic damping. Nevertheless, for practical purposes the results validate the modal work approach.

## 7. Strategies to avoid vortex shedding problems

The most obvious approach to avoid vibration problems by von Karman excitation is to avoid resonance. With sufficiently thick stay vanes and thick trailing edges this could theoretically be achieved. In figure 12a the red curve would have to be shifted below the light-green dashed line of the 1<sup>st</sup> bending mode natural frequency.

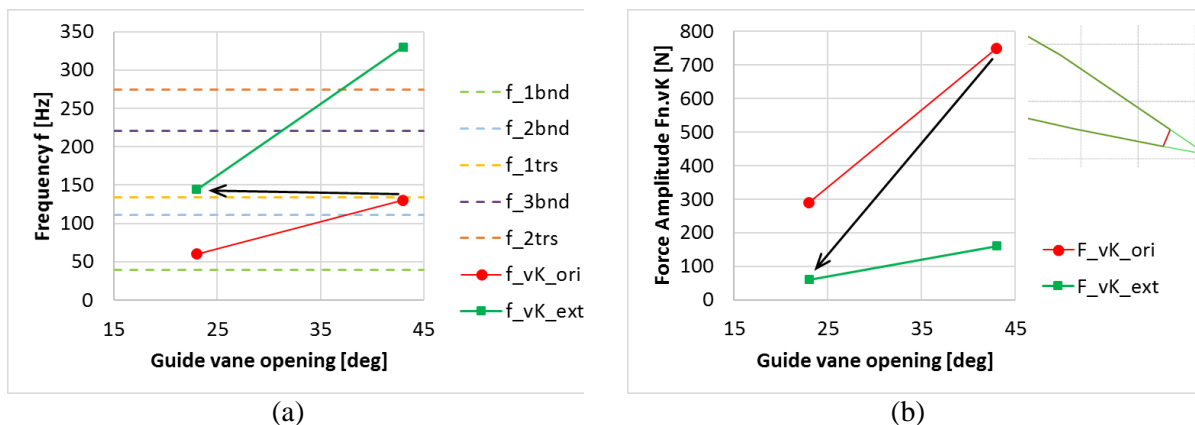


**Figure 12.** Stay vane of an actual low head project with and without trailing edge extension. Left: natural and von Karman frequencies indicating resonance locations. Right: dynamic force amplitudes.

In low head turbines this can lead to hydraulically unacceptable stay vanes. Modern stay vane profiles tend to be hydraulically and mechanically optimized, i.e. profiles are no thicker than necessary with thin trailing edges to avoid wake losses. In such cases, resonance can be unavoidable but need not be problematic. Key is that the vibration amplitude be lower than the permissible vibration amplitude under fatigue considerations. Using the modal work approach, the expected vibration amplitudes can be predicted. If these are higher than the permissible amplitudes, the shedding frequencies can be shifted to higher and the dynamic force to lower values by adding a trailing edge extension as shown in figure

12b resulting in a thinner trailing edge. The example shown in figure 12 is from an actual low head turbine designed by Andritz Hydro. Thinning the trailing edge is beneficial in three ways:

1. Shedding frequency increase – approximately linear with trailing edge thickness – resulting in resonance with higher order, less easily excitable modes.
2. Dynamic force reduction linear with trailing edge thickness and proportional to square of velocity. This can be used to shift intersection of dangerous modes such as 1<sup>st</sup> torsion mode to lower flow and therefore much lower dynamic forcing (black arrows in figure 12) → double benefit in force reduction from thinner trailing edge and lower flow velocity at resonance.
3. No hydraulic disadvantage: same or lower losses, same flow angles.

In the example of the turbine for which frequency and force diagrams are shown in figure 12, the modal work imposing the permissible amplitude was calculated for all stay vane types and modes with risk of resonance. Some of the results showed negative modal work, i.e. expected vibration amplitudes greater than the permissible amplitudes. Stay vane extensions, as shown in figure 12, were then added and equally calculated with the modal work approach. Results for stay vanes with extension showed positive modal work for all cases, i.e. expected vibration amplitudes below permissible amplitudes.

In table 1, results from strain gauge measurements at site during commissioning clearly show that the strategy was successful: actual vibration amplitudes of the modes with resonance are much lower than the permissible amplitudes.

**Table 1.** Comparison of permissible and measured amplitudes on prototype stay vanes.

Type	Mode	Natural Frequency	Permissible Amplitude	Measured Amplitude
[-]	[-]	[Hz]	[mm]	[mm]
II	1 <sup>st</sup> torsion	134.3	0.065	0.008
II	3 <sup>rd</sup> bending	223	0.021	0.002
II	2 <sup>nd</sup> torsion	276	0.035	0.002

The approach of thin trailing edges is also promoted by [14] where they are called “low energy profile”. At Andritz Hydro we prefer to verify that predicted vibration amplitudes are below permissible amplitudes as a final check. As a cautionary note, figure 13 shows that even trailing edges with *1mm* thickness on a large prototype scale stay vane can have sustained natural vortex shedding according to CFD predictions. On the same stay vane a thicker *2.8mm* trailing edge with a different shape was showing no natural vortex shedding, but generated unacceptable noise on the prototype. The modal work approach predicts vibration amplitudes for this *2.8mm* trailing edge exceeding permissible amplitudes. Permissible amplitudes are derived from permissible dynamic stresses under fatigue considerations and depend on a manufacture’s experience. Some very good indications of actual values are given in [6].

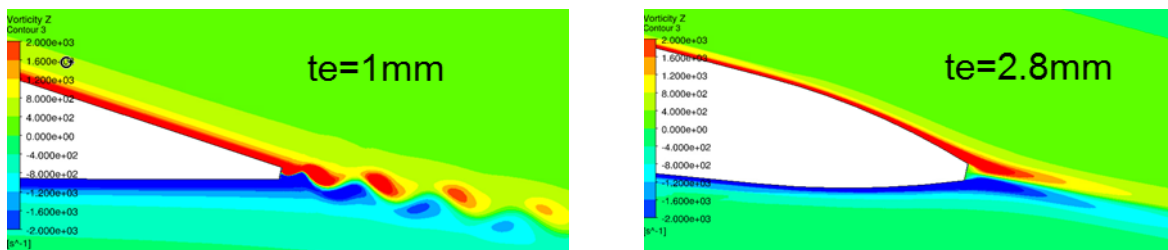


**Figure 13.** Stay vane of a low head project with different trailing edge shapes, unsteady CFD.

## 8. Conclusion

Even today, a risk of unacceptable vibration amplitudes as a result of von Karman vortex shedding on hydraulic profiles – stay vanes in particular – remains. This is due to the fact that structural damping on these profiles is low and hydrodynamic damping under vortex shedding resonance becomes a non-linear function of vibration amplitude. Resonance cannot always be avoided, in particular on stay vanes of high efficiency low head turbines. Therefore it is essential to ensure that vibration amplitudes are lower than permissible amplitudes under fatigue considerations. Our proposed modal work approach to fluid structure interaction permits the reliable prediction of vibration amplitudes under von Karman vortex shedding. Using trailing edge extensions resulting in thin trailing edges is hydraulically beneficial and a suitable strategy to achieve low vibration amplitudes.

## References

- [1] Naudascher E and Rockwell D 2005 *Flow induced vibrations: An engineering guide* Dover Publications Inc. Mineola New York
- [2] Blevins R 2001 *Flow-Induced vibrations* Krieger Publishing Company Malabar Florida
- [3] Heskestad G and Olberts BR 1960 *Influence of trailing-edge geometry on hydraulic-turbine-blade vibration resulting from vortex excitation* J. of Eng. for Power
- [4] Coutu A Proulx D Coulson S 2003 *Dynamic assessment of hydraulic turbines* Waterpower XIII Buffalo NY USA
- [5] Papillon B Brooks J Deniau J-L and Sabourin M 2006 *Solving the Guide Vanes Vibration Problem at Shasta* Hydrovision Portland Oregon
- [6] Gummer JH and Hensman PC 1992 *A review of stayvane cracking in hydraulic turbines* Water Power and Dam Construction
- [7] Lockey K et al 2006 *Flow induced vibrations at stay vanes: Experience at site and CFD simulation of von Kármán vortex shedding* Hydro 2006 Porto Carras Greece
- [8] Dörfler P Sick M Coutu A 2013 *Flow induced Pulsation and Vibration in Hydroelectric Machinery* Springer Heidelberg
- [9] Ausoni P 2009 *Turbulent Vortex Shedding from a Blunt Trailing Edge Hydrofoil* PhD thesis École Polytechnique Fédérale de Lausanne, Switzerland
- [10] Vu TC Nennemann B Ausoni P Farhat M and Avellan F 2007 *Unsteady CFD prediction of von Karman vortex shedding in hydraulic turbine stay vanes* Proceedings Hydro 2007 Spain
- [11] Miyagawa K Fukao S Kawata Y 2004 *Study on stay vane instability due to Vortex shedding* 22th IAHR Symposium on Hydraulic Machinery and Systems, Stockholm
- [12] D'Agostini Neto A Saltara F 2009 *Study of Stay Vanes Vortex-Induced Vibrations with different Trailing-Edge Profiles Using CFD* J. Fluid Machinery and Systems Vol. 2, No. 4
- [13] Alexandre D'Agostini Neto et al 2016 *Engineering diagnostics for vortex-induced stay vanes cracks in a Francis turbine* IOP Conf. Ser.: Earth Environ. Sci. **49** 072017
- [14] Neidhardt T Jung A Heyneck S and Gummer J 2017 *An alternative approach to the von Karman vortex problem in hydraulic turbines* Hydro 2017 Seville Spain
- [15] Coutu A Seeley C Monette C Nennemann B Marmont H 2012 *Damping measurements in flowing water* IOP Conf. Ser.: Earth Environ. Sci. **15** 062060
- [16] Monette C Nennemann B Seeley C Coutu A Marmont H 2014 *Hydro-dynamic damping theory in flowing water* IOP Conf. Ser.: Earth Environ. Sci. **22** 032044
- [17] Nennemann B Monette C Chamberland-L. J 2016 *Hydrodynamic damping and stiffness prediction in Francis turbine runners using CFD* IOP Conf.Ser.: Earth Environ.Sci. **49** 072006
- [18] Yao Z et.al. 2014 *Effect of trailing edge shape on hydrodynamic damping for a hydrofoil* Journal of Fluids and Structures <http://dx.doi.org/10.1016/j.jfluidstructs.2014.09.003i>
- [19] Monette C Coutu A Velagandula O 2007 *Francis Runner Natural Frequency and Mode Shape Predictions* Waterpower XV Chattanooga TN USA
- [20] Zobeiri A 2012 *Effect of Hydrofoil Trailing Edge Geometry on the Wake Dynamics* PhD thesis École Polytechnique Fédérale de Lausanne, Switzerland